

Study of structure formation of transparent spinel-containing glass-ceramic materials for laser techniques

O. Savvova, O. Tur, O. Babich, O. Fesenko, Yu. Smyrnova, I. Tymoshchuk

O.M. Beketov National University of Urban Economy in Kharkiv,
17, Marshal Bazhanov str., Kharkiv, 61002, Ukraine

Received March 18, 2024

The choice was substantiated and compositions of magnesium aluminosilicate glasses for the creation of transparent glass-ceramic materials with a self-organized nanostructure for the obtaining of broadband optical amplifiers were developed. The peculiarities of the structure formation of magnesium aluminosilicate glass-ceramic materials in relation to their light transmission have been studied. The influence of the viscosity of glasses on the nature of phase separation and crystallization under the conditions of low-temperature heat treatment has been established. The mode of heat treatment is selected for obtaining nanostructured spinel-containing glass-ceramic materials for laser technology. The results obtained can be used in the development of bioactive glass-ceramic materials with shortened resorption periods up to one month for the replacement of bone defects.

Keywords: transparent magnesium aluminosilicate glass-ceramic materials, spinel, self-organized structure, structure formation, phase separation, laser technique.

Дослідження формування структури прозорих шпінельвмісних склокристалічних матеріалів для лазерної техніки *О. Саввова, О. Тур, О. Бабіч, О. Фесенко, Ю. Смирнова, І. Тимошук*

Обґрунтовано вибір та розроблено склади магнійалюмосилікатних стекол для створення прозорих склокристалічних матеріалів з самоорганізованою наноструктурою для створення ширококутових оптичних підсилювачів. Досліджено особливості структуроутворення магнійалюмосилікатних склокристалічних матеріалів у взаємозв'язку з їх світлопроникністю. Встановлено вплив в'язкості стекол на характер фазового розділення та кристалізації в умовах низькотемпературної термічної обробки. Обрано режим термічної обробки для одержання наноструктурованих шпінельвмісних склокристалічних матеріалів для лазерної техніки

1. Introduction

The development of modern production leads to the growing introduction of science-intensive technologies, in particular, in the field of laser technology, which received rapid development thanks to modern laser communication systems that contributed to the intensive development of the information society. The global laser technology market size was valued at USD

17.82 billion in 2022 and is expected to expand at a compound annual growth rate (CAGR) of 7.8% from 2023 to 2030 [1].

Effective use of laser radiation sources that generate pulses of short duration (10^{-6} – 10^{-12} s) allow solving complex tasks of telemetry, atmospheric sensing, in information transmission and processing systems.

One of the methods of obtaining laser pulses of short duration is Q-factor modulation us-

ing passive shutters based on light-emitting media. Passive laser gates (saturable absorbers) provide high-power laser pulses without the use of electro-optical Q-factor modulators, which allows for reduced package size and eliminates the need for a high-voltage current source. Common saturable absorber materials are certain ion-doped crystals. For 1- μm lasers (e.g., Nd:YAG), Cr⁴⁺:YAG crystals are mainly used. As chromium ions integrate less well into YAG than neodymium ions, for example, and also exhibit various charge states, the quality of Cr:YAG is unfortunately more variable – particularly if high chromium concentrations are used. This means that choosing a low concentration is preferable, unless there is a clear necessity against it [2, 3]. Absorber crystals for other wavelengths are also available – for example, V³⁺:YAG for 1.3- μm lasers. Typically, these absorber materials have a low saturation fluence (saturation energy per unit area), and their use in focused beams can further reduce the saturation energy (saturation fluence times beam area).

In recent years, single crystals activated by tetrahedrally coordinated divalent cobalt ions [4], in particular single crystals (Co²⁺:MgAl₂O₄, Co²⁺:LiGa₅O₈, Co²⁺:LaMgAl₁₁O₁₉), have attracted special attention as saturable absorbers for Q-factor modulation of solid-state lasers operating in the eye-safe spectral region of about 1.5 μm . In these crystals, cobalt ions have an absorption band in the region of 1.3–1.6 μm , the absorption cross section in which is significantly higher than the cross section of stimulated radiation of erbium ions in active elements based on glasses activated by erbium ions. Therefore, the use of such passive shutters is possible without additional focusing of radiation inside the laser resonator. But the growth of oxide single crystals is complicated by the need to use expensive equipment and equipment under conditions of high temperatures (T_m about 2000 °C), the need to observe the homogeneity of the distribution of the activator in the volume. Alternative transparent ceramic materials are known [5], including those containing the crystalline phase of spinel Co²⁺:MgAl₂O₄ [6]. However, the production of such optical ceramics is also limited by its low optical quality, which prevents its use in laser devices.

Today, the promising application of nanophase glass-ceramics is provided by the set of necessary nonlinear optical, spectroscopic

properties and operational characteristics for the effective use of these materials in lasers in the spectral region safe for vision [7, 8].

There are well-known compositions of transparent glass-ceramic materials based on gahnite and spinel doped with Co²⁺, Cr³⁺, Ni²⁺, Bi³⁺, which are effectively used as broadband optical amplifiers and tunable lasers (Table 1) [9, 10] and for electronic equipment, which are characterized by nonlinear absorption in regions of 1.5–1.6 μm , a high absorption cross section from the ground state, a low saturation energy density, recovery of the initial absorption in about ten to hundreds of nanoseconds, and high radiation resistance [11]. Glass-ceramic materials based on magnesium aluminosilicate glasses have become widely used. Known transparent glass-ceramics are characterized by a high absorption coefficient at 1.54 μm , which is explained by the entry of Co²⁺ ions into the nanoscale crystalline phase in the tetrahedral position. In the experiments, a Co²⁺-doped transparent glass-ceramic sample with a thickness of 0.35 mm was investigated, which was used as a saturated absorber for 1.54 μm laser oscillations on Er-glass, Q-switched pulses with a pulse energy of 40 mJ, a pulse width of 42 ns, and a peak power of 0.95 mW. However, the experimental glass-ceramic material, which was obtained by heat treatment at a temperature of 900 °C for 360 minutes, differed in the content of the crystalline phase no more than 30 vol. % [10].

Known glass-ceramic materials obtained on the basis of MgO–Al₂O₃–SiO₂ (M–A–S) system glasses have a high Vickers hardness of 9–10 GPa and insufficient crack resistance $K_{1C} = 1.1 \text{ MPa m}^{1/2}$ [12]. For use under significant loads, the authors [13, 14] obtained high-strength glass-ceramic materials based on the M–A–S system with a mullite content of 80 vol. %. However, the obtained high-strength materials, although they have short heat treatment times (≈ 2 hours) and high crack resistance $K_{1C} \approx 8 \text{ MPa m}^{1/2}$, are opaque and cannot be used to create optical elements.

The difficulty of obtaining transparent magnesium aluminosilicate glass-ceramic materials is explained by their high melting temperatures of ≈ 1600 – 1650 °C and the duration of two-stage heat treatment at temperatures of 800–900 °C, which affects the increase in the size of crystals of more than 0.4 μm . Therefore, in order to obtain nanostructured transparent glass-ceramic materials under the conditions of

Table 1 – Composition and properties of some transparent glass-ceramics [9, 10]

No	Composition, wt. %	Nanocrystal phase/size	Impurities	Application
1	$x\text{La}_2\text{O}_3$ (1– $x/100$) (14.7MgO, 29.5Al ₂ O ₃ , 47.4SiO ₂ , 5.3TiO ₂ , 3.1ZrO ₂) (x=0, 2.5, 5, 7.5, 10)	MgAl ₂ O ₄ 8.1–10.2 nm	Co ²⁺	Q-switching
2	Yb ₂ O ₃ 1.8, Er ₂ O ₃ 1.7, MgO 11, Al ₂ O ₃ 31.5, SiO ₂ 47, TiO ₂ 4.5, ZrO ₂ 2.5	MgAl ₂ O ₄ 10–20 nm	Co ²⁺	Q-switching
3	SiO ₂ 89, Al ₂ O ₃ 5.9, ZnO 4.9	ZnAl ₂ O ₄ 10–15 nm	Co ²⁺	Laser material in the visible and near-infrared (NIR) regions
4	SiO ₂ 58, Al ₂ O ₃ 10, ZnO 21, K ₂ O 3, Ga ₂ O ₃ 3, TiO ₂ 5	ZnAl ₂ O ₄ 10–15 nm	Ni ²⁺	Broadband optical amplification
5	SiO ₂ 39.3, Al ₂ O ₃ 26.7, ZnO 21.3, TiO ₂ 6.3, ZrO ₂ 6.4	ZnAl ₂ O ₄ 11.5 nm	Cr ³⁺ / Ni ²⁺	Broadband optical amplifier and tunable lasers
6	(100-x)(55SiO ₂ –18Al ₂ O ₃ –18MgO–9TiO ₂)–xGa ₂ O ₃) (x=0, 2.5, 5, 7.5, 10) mol. %	MgAl ₂ O ₄ 7.6 nm	Ni ²⁺	Broadband optical amplifier and tunable lasers
7	(100-y) (16.7MgO · 16.7Al ₂ O ₃ · 8.3Ga ₂ O ₃ · 50SiO ₂ · 8.3TiO ₂ · xNiO) _y Bi ₂ O ₃ (y=0, 0.25, 0.5, 0.75, 1, where x=0) mol. %	MgAl ₂ O ₄ 6 nm	Ni ²⁺ / Bi ³⁺	Broadband optical amplifier and tunable lasers
8	51SiO ₂ –24.5Al ₂ O ₃ –23MgO–1.5K ₂ O doped with 0.5 wt% Co(NO ₃) ₂ and doped with 4 wt.% and 6 wt.% additional nucleating agents ZrO ₂ and TiO ₂	MgAl ₂ O ₄ ZrTiO ₄	Co ²⁺	Q-switching

low-temperature high-speed heat treatment, it is important to study the processes of structure formation in magnesium aluminosilicate glasses at the initial stages of nucleation and the formation of an optical volumetric sitalized structure, which determines the relevance of this work.

2. Experimental

2.1. Aim setting and research methodology

The aim of the work is to study features of the structure formation of the glasses in the MgO–Al₂O₃–SiO₂ system during heat treatment.

To achieve the aim, the following tasks were set:

1. Establishment of a set of criteria for glass as the basis of a transparent glass-ceramic material based on spinel;
2. Substantiation of the glass composition choice for obtaining a transparent glass-ceramic material;
3. Determining the glass viscosity influence on the crystallization ability of experimental glasses;
4. Establishment of the mechanism of structure formation of magnesium aluminosilicate materials during heat treatment in relation to light transmission;

5. Selection of technological parameters for obtaining transparent glass-ceramic material.

The crystallization ability of glasses was assessed by the methods of petrographic (EMV 100 AK microscope) and X-ray phase (DRON-3M diffractometer) analyses. The structure of the glasses was studied by electron microscopy (scanning electron microscope SEM with a maximum resolution of 1 nm). The viscosity of the experimental glasses was studied by the thread elongation method. The light transmittance of glass-ceramic materials was determined using a FM-94M photometer.

2.2 Establishment a set of criteria for the glass matrix as the basis of transparent glass-ceramic materials

The choice of a system for obtaining transparent glass-ceramic materials was based on the fundamental principles of designing nanostructured glass-ceramic materials, taking into account the requirements for the materials on chemical composition and properties.

The combination of high operational properties of transparent magnesium aluminosilicate glass-ceramic materials as the basis for materials of Q-switches can be ensured by the formation of a sitalized self-organized nanostructure of the glass matrix during heat treatment due to the ability to:

- the formation of a significant number of composition and structure fluctuations and, based on them, stabilized clusters, which are ordered due to metastable phase separation through the spinodal mechanism during supercooling of the glass melt in the M–A–S system;
- formation of structurally formed sybotaxic groups $[\text{AlO}_4]^{6-}$ at temperatures below t_g in a glass melt with a viscosity of $\approx 10^8$ Pa s;
- the flow of relaxation processes of nucleation and crystallization in the interval of low temperatures (800 – 1000 °C) during short heat treatment;
- formation of nanosized spinel doped with cobalt cation.

It is important to study the phase separation in glasses and its influence on the structure formation of glass-ceramic materials during heat treatment [15]. Let us consider in detail the processes of the structure formation of magnesium aluminosilicate glass for which, upon reaching the solidus temperature t_s , the formation of solid solutions takes place, the chemical composition of which is identical to the chemical composition of the original melt. In these glasses, during crystallization, a solid solution with a chemical composition similar to glass is formed, and in the liquid melt there is a complete “mixing” with respect to the structural elements of the limiting stoichiometric crystals, so that the most distorted lattices (structural elements) of the melt near the liquidus temperature have some mixed structure, similar to the structure of a solid solution. The structures of melts that crystallize with disintegration into crystals of different composition x and y , which are close to stoichiometric D and B are presented in Fig. 1.

For glass melts of the M–A–S system, recrystallization through the melt of the solid solution x' into more refractory forms with a composition that shifts in the direction of the crystalline phase D should occur between the solidus t_s and liquidus t_L temperatures. As the temperature increases, the average structure of the crystal lattice also changes, which are in equilibrium with the melt and the lattice structure of the melt. At temperatures above the liquidus temperature (t_L), we should expect an increase in the number of structural elements characteristic of crystals A and B. In Figure 1, the liquation maximum is smoothly extended by a dashed line below the liquidus line L and even the solidus S. This entire area is a zone of metastable liquation, which flows in the su-

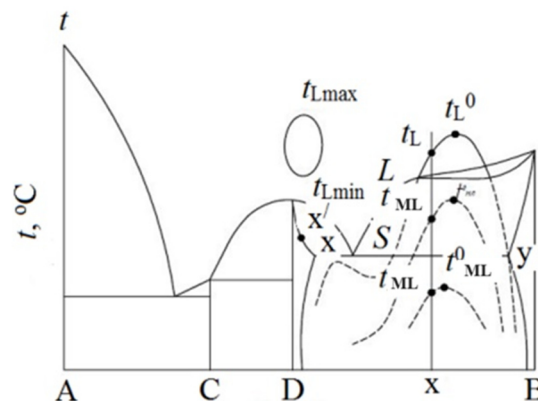


Fig. 1. Phase diagram of the A–B binary system

percooled melt, which, like the liquid phases formed during liquation, is metastable, is unstable with respect to crystallization. Above the solidus line S , liquid liquation phases are unstable with respect to the crystallization of phase A, below the line – with respect to the crystallization of phases B and D (or x and y). If the tendency to aggregation of homogeneous structural elements x and y is not expressed strongly enough, then the liquation on the diagram may be below the liquidus line and even below the solidus line, and even be absent, since the critical structure for the appearance of metastable liquation t_{ML}^0 (if it exists) is too low ($t_{ML}^0 < t_g$).

2.3 Choice of compositions and synthesis of glass materials

For the formation of a dissipative nanostructure, it is necessary to create a significant number of stabilized clusters above the liquidus temperature and ensure the occurrence of metastable spinodal liquation, which is more energetically beneficial for volumetric crystallization in experimental glasses.

Thanks to the regulation of the nucleation energy, crystallites in glass-ceramics can self-organize into heteronanodomains during the solid-phase reaction [16].

The content of TiO_2 , ZrO_2 and $\text{TiO}_2 + \text{ZrO}_2$ and the ratio of phase-forming components $\text{SiO}_2/\text{Al}_2\text{O}_3$ and $\text{MgO}/\text{Al}_2\text{O}_3$ are of particular importance for the structure formation of glass-ceramics [17, 18]. For experimental glasses, along with the presence of P_2O_5 , a significant content of ZnO [18–21], CaO , and MgO enhances liquation separation, while the size and number of droplets increases. SrO and BaO , as cations with a large ionic radius, on the contrary, lead to inhibition of liquation, while the

Table 2 – Characteristics of chemical composition of glasses and content of crystalline phase in the composition of glass-ceramic materials after heat treatment according to modes 1 and 2 and the value of light transmission (T)

Group of glasses	Marking	Characteristics of chemical composition						Type and content of the crystalline phase (vol.%) after the 1st mode of heat treatment	T, %	Type and content of the crystalline phase (vol.%) after the 2nd mode of heat treatment
		MgO	Al ₂ O ₃	SiO ₂	ZnO, TiO ₂ , CeO ₂ , ZrO ₂ , P ₂ O ₅	BaO, SrO, CaO	CoO			
I	PSK-1	4	20	57	14.7	3	0.3	spinel – 10 α-quartz – 20 mullite – 20	.*	α-cordierite – 65 mullite – 20
	PSK-2	8	19	58	10.7	3	0.3	spinel – 10 α-quartz – 20 mullite – 20	.*	α-cordierite – 40 mullite – 20 spinel – 10 α-cristobalite – 10
	PSK-3	12	20	57	7.5	2.2	0.3	mullite – 20 spinel – 20 α-quartz – 10	.*	mullite – 40 cristobalite – 20 spinel – 10
	PSK-4	10	25	54	15	1.9	0.1	cristobalite – 20	.*	α-cristobalite – 85
II	PSK-5	12	20	45	10	1.9	0.1	spinel – 20 α-quartz – 10	.*	mullite – 20 spinel – 10
	PSK-6	9	30	45	9.9	1	0.1	mullite – 20 spinel – 20 α-quartz – 10	.*	mullite – 80
	PSK-7	10	30	50	7.9	2	0.1	spinel – 40 α-cristobalite – 20	50	α-cordierite – 80
	PSK-8	10	35	45	6.9	2	0.1	spinel – 20 α-cristobalite – 10	70	α-cordierite – 20
	PSK-9	15	30	45	6.9	2	0.1	spinel – 20 α-quartz – 10	70	α-cordierite – 30
	PSK-10	15	25	50	4.9	1	0.1	spinel – 40 α-quartz – 10	72	α-cordierite – 70
	PSK-11	10	25	50	6.4	2	0.1	spinel – 20 α-quartz – 10	70	α-cordierite – 40

* opaque material

number and size of drops decrease. Therefore, when the ionic radius increases in the series MgO>CaO>SrO>BaO, the degree of liquid phase separation decreases.

At the same time, it is important to ensure metastable phase separation, which occurs under conditions of increased viscosity in the glass transition interval, which leads to the formation of a developed droplet biframe structure in a short time [20]. The viscosity of the glass melt of the M–A–S system increases with an increase in the concentration of CeO₂ and ZrO₂, while an increase in the content of CeO₂ can lead to a decrease in the content of cordierite. In general, the addition of oxides of rare earth elements to cordierite glass-ceramics of non-stoichiometric composition will reduce the

sintering temperature to 900–950 °C and improve the densification process and reduce the sintering activation energy. It should be noted that the tendency to crystallization when replacing some oxides with others decreases with an increase in the viscosity of the glass in the crystallization temperature range. It should be taken into account that magnesium-containing glasses have the lowest viscosity during production. They also have the smallest temperature range of viscosity reduction. Calcium and strontium oxides are used along with B₂O₃ to reduce viscosity at high temperatures and melting point, increase tensile, compressive and bending strength. In general, the influence of RO oxides on reducing viscosity and, accordingly, on the melting time of glasses increases in the following sequence: BaO<SrO<CaO<ZnO<MgO.

Taking into account the specified criteria, compositions with PSK marking in the MgO–ZnO–CaO–SrO–BaO–CoO–ZrO₂–TiO₂–CeO₂–Al₂O₃–B₂O₃–P₂O₅–SiO₂ system were designed for the glass matrix, which are characterized by different contents of phase-forming oxides MgO, Al₂O₃ and SiO₂ content (Table 2) for the crystallization of spinel, as a crystalline phase that provides high light transmission and mechanical strength.

Experimental glasses with PSK marking in the experimental system were melted in corundum crucibles at temperature range of 1550–1650 °C in condition of oxidising atmosphere. In order to crystallization of spinel, the experimental glasses were processed at temperatures of nucleation T₁ and growth of crystals T₂ according to mode 1 (T₁=850 °C and T₂=1000 °C) and mode 2 (T₁=850 °C and T₂ = 1150 °C) for 2 hours at each stage for the purpose of identifying crystalline phases by X-ray phase and petrographic analysis methods.

2.4 Study of phase formation in magnesium aluminosilicate glasses during heat treatment

The crystallization process in magnesium aluminosilicate glasses proceeds through the formation of intermediate phases and can be represented by the following scheme of phase transformations: glass → 800–1000 °C (solid solutions + MgO·Al₂O₃+ 4MgO·5Al₂O₃·2SiO₂) → >1100 °C (mainly α-cordierite and solid solutions) → >1150–1200 °C (mullite).

However, the change in the disproportionation mechanism of stoichiometric cordierite to spinel and silica up to 1227 °C and to sapphirine and silica at a higher temperature and the influence of the glass phase and possible additional oxides on the course of the reactions require further studies of the crystallization features of glasses in the M-A-S system.

The peculiarity of PSK-1, PSK-2, PSK-3 glasses of group I, which belong to the high-silica region with a SiO₂ content > 50 wt. %, is the presence of a crystalline phase of mullite already after melting in the amount of 30 wt. %, which will contribute to the intensification of phase formation in experimental glasses with the subsequent growth of crystals > 1 μm when the temperature is increased to 1000 °C. This leads to the formation of solid solutions based on high-temperature quartz, spinel, and mullite in the amount of 50% in the structure of experimental glasses and their opacification during heat treatment according to mode 1. PSK-4

glass after melting is transparent and retains opalescence up to 1000 °C with the presence of α-cristobalite. For this glass, beginning at 900 °C, α-quartz intensively transforms into α-cristobalite. When the heat treatment temperature for these glasses is increased > 1000 °C, the rate of crystallization of cordierite primarily depends on the amount of mullite formed after melting, since the formation of nuclei accelerates the crystallization of cordierite.

Volumetric finely dispersed crystallization with a crystalline phase content of 70–85 vol. % with a predominant α-cordierite content of 40–65 vol. %, mullite 20–40 vol. % and spinel 10 vol. % is characteristic of the glasses of the I group, when mode 2 is implemented (Table 2). For experimental glasses, the temperature increase to 1050 °C leads to cordierite first formation from mullite as a result of the reaction: A₃S₂·2MA + 3S = 3A + M₂A₂S₅, which, when the temperature is increased to 1150 °C, interacts with alumina to form mullite and spinel according to the reaction: 15A + 2M₂A₂S₅ = 4MA + 5A₃S₂, which is consistent with data [13]. The thermodynamic stability of cordierite is ensured in the low-temperature range (up to 927 °C) by the reaction 4MA + A₃S₂ = 15A + M₄A₄S₁₀; then (up to 1227 °C) by the reaction A₃S₂ + M₄A₅S₂ = 12A + M₄A₄S₁₀ [13].

For glasses of group II, which are transparent after melting, during heat treatment according to mode 1, crystallization of α-quartz and spinel occurs in the amount of 30 to 50 vol. % with a predominant content of spinel, which correlates with the light transmission of materials, which decreases with an increase in the content of the crystalline phase (Table 2). The formation of solid solutions based on α-cordierite according to mode 2 is realized in these glasses due to chemical interaction according to the reaction: 2MA + 5S = M₂A₂S₅. According to petrographic analysis, sapphirine, which is disproportionate to spinel and silica, is not fixed in the structure of glasses during heat treatment. This indicates the speed of the reaction 4MA + A₃S₂ = 3A + M₄A₅S₂ with the participation of sapphirine and is extremely important for the self-organization of the structure of materials. Taking into account the possibility of ensuring light transmission during the formation of a self-organized structure followed by volumetric crystallization of spinel the glasses of group II were selected for further research.

2.5 Study of the viscosity influence on the mechanism of structure formation in glasses

In order to obtain a uniform fine-crystalline structure of sitall, it is necessary to create a high concentration of evenly distributed crystalline nuclei in the glass in a significant amount. It is obvious that the pre-crystallization metastable phase separation of supercooled glass melt with the formation of phase separation boundaries initiates the formation of nuclei. Metastable liquation of glass is a special state of a non-equilibrium system with separated glassy phases (droplet and matrix), their compositions are close to crystalline phases or eutectics, in the crystallization fields of which liquation occurs. The uniformity of the distribution of nuclei, their number and size in the glass depend on the rate of cooling of the melt and the rate of diffusion of ions. At low temperatures, the high viscosity of the melt and insufficiently intensive movement of ions lead to a decrease in the size of the liquation regions and an increase in their number.

The confirmation of the metastable phase separation in experimental glasses of the PSK series is that these processes take place relatively slowly in conditions of increased viscosity of both the original melts and crystalline phases in a narrow temperature range (Fig. 2).

The growth of the crystallization viscosity $\eta = 10^{7.7-10^{8.2}}$ Pa·s in the temperature range of 750–800 °C for the experimental glasses of the PSK series of the group II indicates both the intensive formation of nucleators and the growth of crystals (Fig. 2). The high viscosity of glass determines the important contribution of the kinetics of the process: in the time available for observation, the glass cannot be divided into two layers, the glass phase that is released forms finely dispersed droplets, and this leads to the formation of a developed droplet biframe structure in a short time [22]. Anomalous increase in viscosity at elevated temperature in the glass transition interval $T_g - T_f$ for glasses that are capable of sitallization is associated with a high rate of temperature increase in the area of the glass transition interval, which precedes the increase in viscosity, which leads to a dip in the curve in viscosity. This state is quickly eliminated, because in the new temperature conditions there is a more intense increase in the crystalline phase due to a decrease in the amount of glassy phase, which determines the repeated increase in viscosity before the end

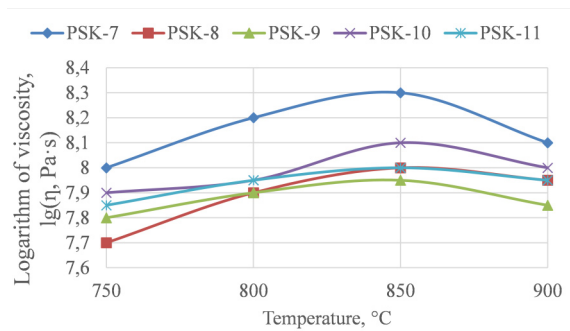


Fig. 2. Viscosity of experimental glasses

of heat treatment [22]. At a temperature of 850 °C, the maximum increase in viscosity is observed, which is $10^{7.9-10^{8.3}}$ Pa·s. For the formation of a sitallized structure, such a course of the curve of viscosity dependence on temperature should be considered optimal, when its maximum is shifted to the temperature range below the softening point, that is, to the range of viscosity values above 10^8 Pa·s. It is more important that at low temperatures, the high viscosity of the melt and the insufficiently intensive movement of ions lead to a decrease in the size of the liquation regions, an increase in their number, and a shift in their appearance to the region near T_g . These data not only determine the dependence of the sample viscosity change as a function of crystallization, but also determine the direction of controlling the thermal history during crystallization to manage the optical properties of materials.

The difference in the nature of the viscosity curve for PSK-10 glass is that the formation of fluctuations is observed at a viscosity from $10^{7.9}$ to $10^{8.1}$ Pa·s in the temperature range of 750–850 °C, which is realized due to a decrease in the content of ΣTiO_2 and $\text{ZrO}_2 = 1$ wt. % and the content of $\text{SiO}_2 = 50$ wt.%, which is an important factor in limiting the growth and appearance of new types of crystals, which are different in properties from the main crystals.

In order to determine the formation of the structure at the initial stages of nucleation, PSK-10 glass was chosen, which is characterized by the highest light transmission (72%) and spinel content (40 vol.%) (Table 2). The following characteristic temperatures were chosen: the temperature in the phase separation region t_1 ; temperature in the region of nucleation t_2 ; temperature of appearance of the first crystalline phase t_3 ; final crystallization temperature t_4 . To identify the structure of the glass material at the initial stages of nucleation, areas free from crystallization were selected. The du-

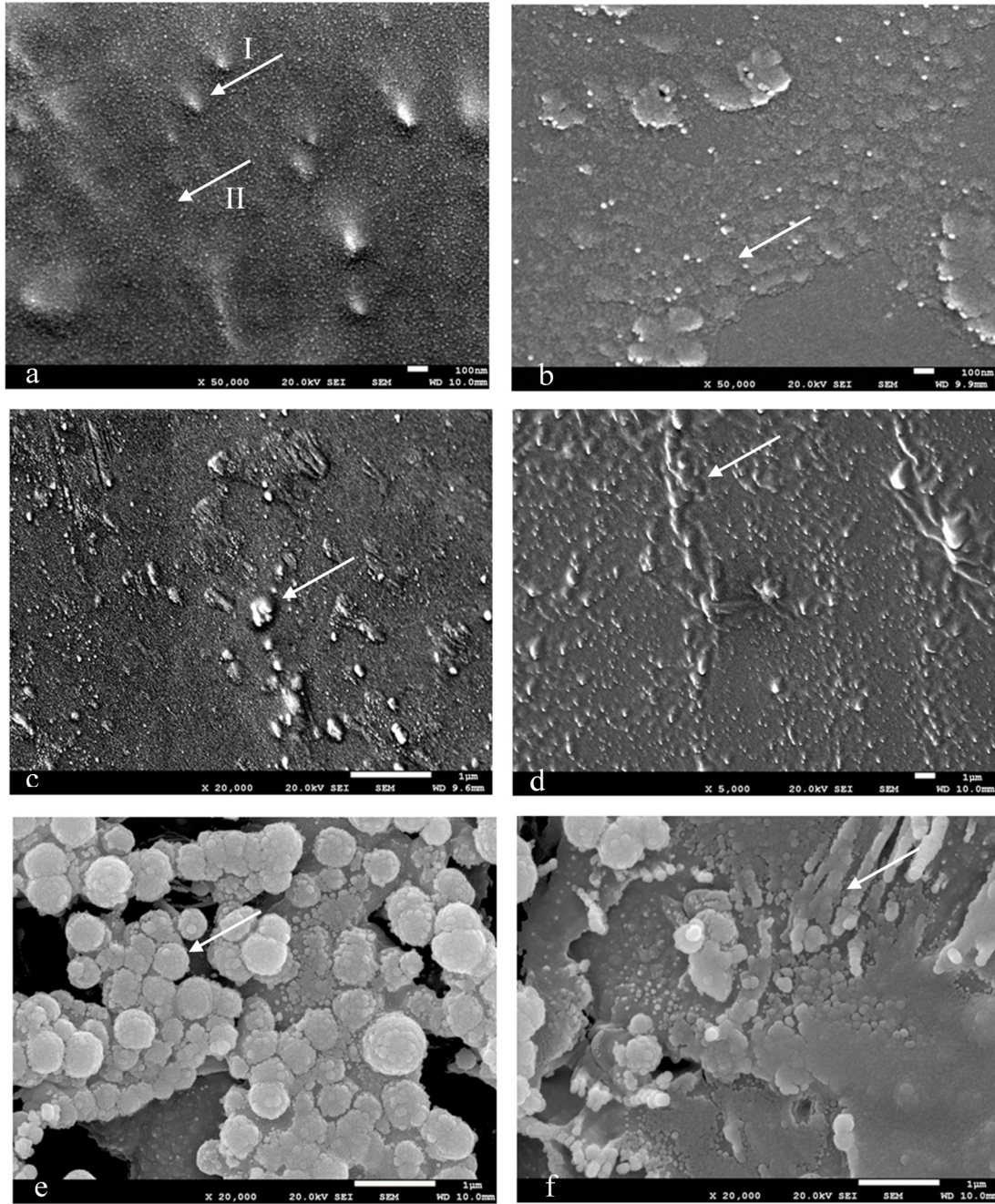


Figure 3 – Structure of PSK-10 experimental glass-ceramic material during heat treatment: a – 800 °C; b – 850 °C; c, d – 900 °C; e – 950 °C; f – 1000 °C

ration of exposure of the experimental samples at each stage was 0.5 h.

According to the results of electron microscopy, the PSK-10 glass material at $t_1 = 800$ °C represents a multiphase system formed from the mother glass, with spherulites ≈ 50 nm in size (Fig. 3 a, I) with clearly defined boundaries and densely placed inhomogeneities of 10 nm in the material structure (Fig. 3 a, II), which may be nuclei of crystallization. An important

influence on the uniformity of the distribution of crystals, their number is ≈ 50 vol. % and nanoscale in glass, has a cooling rate of the melt and a rate of diffusion of ions.

It is obvious that the pre-crystallization metastable phase separation of supercooled glass melt significantly affects the formation of phase boundaries and the formation of nano-sized crystals. The formation of a significant number of spherulites prevents the further

growth of crystals $> 0.4 \mu\text{m}$ at increasing temperatures, which can lead to a decrease in light transmission. At low temperatures, high viscosity reduces the intensity of diffusion and inhibits the growth of crystalline phases and the formation of new crystalline phases different in composition from the main phase.

When the temperature is increased to $t_2 = 850 \text{ }^\circ\text{C}$, the growth of nanoinhomogeneities in the glass structure and their combination in ridges 100-200 nm in size and the formation of crystallization nuclei on their faces are observed. This self-organization of the structure is characteristic of phase separation by the spinodal mechanism and is manifested in the presence of nanoinhomogeneities of the order of 100 nm, which form spherical rings 50-100 nm in size (Fig. 3 b), which merge and aggregate into aggregates with clear boundaries (Fig. 3 c) when the temperature rises to $900 \text{ }^\circ\text{C}$ against the background of a dense structure of inhomogeneities (Fig. 3 d). It is due to spinodal phase separation with a decrease in the free energy of the system as a result of low-temperature heat treatment of glass that thermodynamically favorable conditions are created for the appearance of a significant number of composition fluctuations, followed by the formation of a significant number of nanocrystals. It is important that the composition of nano-sized crystals of quartz-like solid solutions and matrix magnesium aluminosilicate glass are similar, therefore, in the formed heterogeneous system, sharp boundaries of the separation of two phases are not formed, which is important for ensuring the light transmission of the material due to the approximation of the refractive indices of the crystalline and glass phases [23].

The intensification of the formation of solid solutions with the structure of high-temperature quartz and spinel is observed when the temperature rises to $t_3 = 950 \text{ }^\circ\text{C}$, more developed crystals are formed, which are evenly distributed (Fig. 3 e). The self-organization of spherical inhomogeneities of 100 nm into spherical aggregates with clear architecture along the planes is characteristic of the research material. The combination of these aggregates with each other and merging into drusen is observed. Such twins along the (111) planes are characteristic of spinel, which crystallizes in cubic syngonia and occurs in the form of octahedra or flat triangular plates bifurcated at the corners. The expressiveness of the change in the structure of the experimental glass is explained by the

possibility of realizing many stationary states of the structure during the thermal evolution of the phase composition of magnesium aluminosilicate glasses in the M–A–S system with the possibility of a reverse solid-phase reaction of the exchange type [24].

Further structural self-organization at an increase in temperature to $t_4 = 1000 \text{ }^\circ\text{C}$ leads to a decrease in the size of inhomogeneities and their merging, alignment of the structure, and formation of the faces of spinel crystals of an octahedral habit (Fig. 3 f). This indicates the possibility of obtaining, on the basis of experimental glass the glass-ceramic material with a high concentration of uniformly distributed crystalline nuclei of crystallization. The regular nature of the distribution of nanocrystals in the residual glass phase leads to interference effects in the process of scattering X-rays and visible light, which creates conditions for obtaining a highly transparent glass-ceramic material.

Taking into account the conducted research and previous studies on the development of transparent glass-ceramic materials, the following heat treatment mode was chosen for obtaining transparent nanostructured spinel-containing glass-ceramic materials: (I st. – $T = 800 \text{ }^\circ\text{C}$, $\tau = 30 \text{ min}$; II st. – $T = 900 \text{ }^\circ\text{C}$, $\tau = 30 \text{ min}$, III st. – $T = 1000 \text{ }^\circ\text{C}$, $\tau = 5 - 15 \text{ min}$).

4. Conclusions

The peculiarities of compositions and properties of glass-ceramic materials for passive laser shutters were analyzed. A set of criteria has been established for the glass matrix as the basis of transparent glass-ceramic materials. The choice was substantiated and compositions of magnesium aluminosilicate glasses with a defined content of phase-forming and modifying components were developed. The regularities of the structure formation and phase composition of magnesium aluminosilicate glasses under the conditions of high-speed low-temperature heat treatment have been established, which consist in the following sequential processes: the formation of composition fluctuations when providing $\sum \text{Al}_2\text{O}_3, \text{MgO} = 40 \text{ wt. } \%$ and content of $\text{SiO}_2 = 50 \text{ wt. } \%$ by phase separation according to the spinodal mechanism ($T = 800 \text{ }^\circ\text{C}$); self-organization of the structure by the formation of nucleators at $\eta = 10^{8.0} \text{ Pa}\cdot\text{s}$, which merge into ridges and interpenetrating phases with a content of $\approx 50 \text{ vol. } \%$ ($T = 850 \text{ }^\circ\text{C}$; $\tau = 0.5 \text{ h}$); formation of solid solutions with the structure of high-

temperature quartz and spinel ($T=900\text{--}950\text{ }^{\circ}\text{C}$; $\tau=0.5\text{ h}$); formation of a dissipative sintered structure due to nanostructuring with the presence of spinel of an octahedral habit ($T=1000\text{ }^{\circ}\text{C}$, $\tau=10\text{ min}$). The technological parameters were chosen for obtaining a transparent glass-ceramic material based on spinel were selected and nanostructured sintered with a light transmission of 72% and with a content of 40 vol. % of submicron spinel crystals as a basis for functional elements of optics and laser technology.

References

1. Laser Technology Market Size, Share & Trends Analysis Report By Type (Solid-state Lasers, Gas Lasers, Liquid Lasers, Semiconductor Lasers), By Product, By Application, By Vertical, By Region, And Segment Forecasts, 2023 – 2030. Grand View Research (2023).
2. H.H. Lim and T. Taira, *Opt. Express*, **27**, 31307 (2019). <https://doi.org/10.1364/OE.27.031307>
3. T. Chen, X. Chen, C. Zhou et al., *Appl. Opt.*, **59**, 4191 (2020). <https://doi.org/10.1364/AO.391180>
4. S. Nizhankovskiy, A. Kozlovskiy, O. Vovk et al., *Acta. Phys. Pol. A*, **141**, 371 (2022). <https://doi.org/10.12693/APhysPolA.141.371>
5. Z. Xiao, S. Yu, Y. Li et al., *Mater. Sci. Eng. R Rep.*, **139**, 100518 (2019). <https://doi.org/10.1016/j.mser.2019.100518>
6. S. Su, Q. Liu, Z. Hu et al., *J. Alloys. Compd.*, **797**, 1288 (2019). <https://doi.org/10.1016/j.jallcom.2019.04.322>
7. C. Goyes, E. Solarte, S. Valligatla, in: International Conference on Transparent Optical Networks (ICTON), Budapest, Hungary (2015), p. 1. <https://doi.org/10.1109/ICTON.2015.7193488>
8. B. Karmakar, *Functional Glasses and Glass-Ceramics: Processing: Properties and Applications*. Elsevier. Ins. (2017).
9. V. Marghussian *Nano-Glass Ceramics: Processing, Properties and Applications*. Elsevier. Ins. (2015).
10. S.Y. Feng, C.L. Yu, L. Chen et al. *Laser Phys.*, **20**, 1687 (2010). <https://doi.org/10.1134/S1054660X10150089>
11. U.S. Patent 11,192,818.
12. L. Sant'Ana Gallo, F. Célerié, J. Bettini et al. *Ceram. Int.*, **48**, 9906 (2022). <https://doi.org/10.1016/j.ceramint.2021.12.19>
13. O.V. Savvova, S.M. Logvinkov, O.V. Babich, and A.R. Zdorik. *Voprosy Khimii i Khimicheskoi Tekhnologii*, **3**, 96 (2018).
14. O. Savvova, O. Babich, V. Tymofeev et al. *Functional Materials*, **29**(2), 228 (2022). <https://doi.org/10.15407/fm29.02.228>
15. J.M. Bussey, M.H. Weber, N.J. Smith-Gray et al. *J. Non. Cryst. Solids*, **600**, 121987 (2023). <https://doi.org/10.1016/j.jnoncrysol.2022.121987>
16. Y. Wang, H. Qu, B. Liu et al. *Nat. Commun.*, **14**(1), 669 (2023). <https://doi.org/10.1038/s41467-023-35982-7>
17. Z. Pei, H. Huang, X. Guo et al. *Crystals*, **13**(8), 1261 (2023). <https://doi.org/10.3390/cryst13081261>
18. B. Li, K. Jing, and H. Bian. *J. Non-Cryst. Solids*, **500**, 487 (2018). <https://doi.org/10.1016/j.jnoncrysol.2018.09.006>
19. L. Cormier, L. Delbes, B. Baptiste, and V. Montouillout. *J. Non-Cryst. Solids*, **555**, 120609 (2021). <https://doi.org/10.1016/j.jnoncrysol.2020.120609>
20. B. Mirhadi, B. Mehdikhani, and N. Askari. *Solid State Sci.*, **14**(4), 430 (2012). <https://doi.org/10.1016/j.solidstatesciences.2012.01.010>
21. G.H. Chen. *J. Mater. Sci.: Materials in Electronics*, **18**(12), 1253. <https://doi.org/10.1007/s10854-007-9283-8>
22. O.V. Savvova, G.K. Voronov, O.V. Babich et al. *Functional Materials*, **26**(1), 182 (2019). <https://doi.org/10.15407/FM26.01.182>
23. O.V. Savvova, G.K. Voronov, V.L. Topchiy, and Yu.O. Smyrnova. *Chem. Chem. Technol.*, **12**(3), 391 (2018). <https://doi.org/10.23939/chcht12.03.391>
24. O. Savvova, H. Voronov, O. Fesenko et al. *Chem. Chem. Technol.*, **16**(2), 337 (2022). <https://doi.org/10.23939/chcht16.02.337>